nature neuroscience

Neural activity at the human olfactory epithelium reflects olfactory perception

Hadas Lapid[1,2], Sagit Shushan[1,3], Anton Plotkin[1], Hillary Voet[4], Yehudah Roth[3], Thomas Hummel[5], Elad Schneidman[1] & Noam Sobel[1]

Organization of receptive surfaces reflects primary axes of perception. In vision, retinal coordinates reflect spatial coordinates. In audition, cochlear coordinates reflect tonal coordinates. However, the rules underlying the organization of the olfactory receptive surface are unknown. To test the hypothesis that organization of the olfactory epithelium reflects olfactory perception, we inserted an electrode into the human olfactory epithelium to directly measure odorant-induced evoked responses. We found that pairwise differences in odorant pleasantness predicted pairwise differences in response magnitude; that is, a location that responded maximally to a pleasant odorant was likely to respond strongly to other pleasant odorants, and a location that responded maximally to an unpleasant odorant was likely to respond strongly to other unpleasant odorants. Moreover, the extent of an individual's perceptual span predicted their span in evoked response. This suggests that, similarly to receptor surfaces for vision and audition, organization of the olfactory receptor surface reflects key axes of perception.

Receptive surfaces have evolved to optimally encode the sensory scene. Thus, their organization typically reflects key perceptual axes relevant to their function. For example, vision is spatial, and retinal coordinates reflect spatial coordinates[1]. Audition is tonal, and cochlear coordinates reflect tonal coordinates[2]. In contrast, the perceptual axes of olfaction are poorly understood, and organizational coordinates of olfactory epithelium have yet to be linked to perception.

In rodents, the ~1,200 olfactory receptor subtypes are spatially segregated in four zones along a dorso-ventral epithelial axis, grouped by gene subfamily[3]. Although initial observations suggested that receptor subtypes are randomly distributed in each zone, later observations revealed both zonal overlap[4] and non-stochastic organization in a zone[5]. The functional importance associated with the dorso-ventral zonal organization, as well as its persistence across mammalian species, is unclear. For example, humans express ~12 million copies[6] of ~400 intact receptor subtypes[7], and very little is known regarding their spatial distribution in the adult nose.

Although several expression studies in rodents have suggested that receptor subtypes are randomly distributed in a zone, most functional studies have found potential order in the organization of the olfactory receptive surface. Such order was first suggested by the finding that precisely directing the same odorant at different portions of the epithelium generates different response patterns at the bulb[8]. Moreover, directly measuring epithelial response both electrically and optically revealed odorant-dependent spatial patterns of epithelial activation[9–14]. These patterns may be partly imposed, reflecting a chromatographic-like interaction of odorant sorption and clearance in the mucosa[15,16], and partly inherent, reflecting meaningful topographical dispersion of receptor subtypes as a function of their tuning curves[12]. However, whether imposed, inherent or a combination of both, the axes underlying this order remain unknown.

A large body of research has suggested that odorant pleasantness is the primary perceptual axis of human olfaction[17–21]. Note that the term pleasantness is used here to describe an axis ranging from very unpleasant to very pleasant, an axis that is also referred to as odor valance, or odor hedonic tone. Recently, we linked this axis to odorant structure[19] and to neural responses obtained (by others[22]) in human olfactory receptors *in vitro*[23]. Given that single olfactory receptor subtypes reflect perception[24], we set out to test the hypothesis that in olfaction, similarly to other distal senses, receptors are grouped in accordance with a key perceptual axis, namely pleasantness.

There are two approaches to examining the organization of a receptive surface. One is to keep the stimulus constant and to systematically span the receptive surface. The second is to keep the location at the receptive surface constant and to systematically span the stimulus space. Ideally, one would use both approaches. However, because the human olfactory epithelium is a highly variable and convoluted structure, whose boundaries cannot be determined by endoscopic guidance[25], we used the second approach alone. We placed an electrode at a responsive location on the upper portions of the middle turbinate (**Fig. 1a–c**) and recorded an odorant-induced sum of generated potentials referred to as an electro-olfactogram (EOG; **Fig. 1**)[26]. We then delivered odorants selected to span stimulus space. We found that different recording sites were differently tuned, implying that dispersion of receptor subtypes is not both uniform and random. Moreover, distances in the EOG response correlated with distances

[1]Department of Neurobiology, Weizmann Institute of Science, Rehovot, Israel. [2]Department of Computer Science and Applied Mathematics, Weizmann Institute of Science, Rehovot, Israel. [3]Department of Otolaryngology-Head and Neck Surgery, Edith Wolfson Medical Center, Tel-Aviv University Sackler School of Medicine, Holon, Israel. [4]Robert H. Smith Faculty of Agriculture, Food and Environment, Hebrew University of Jerusalem, Rehovot, Israel. [5]Smell and Taste Clinic, University of Dresden Medical School, Dresden, Germany. Correspondence should be addressed to H.L. (hadas.lapid@gmail.com) or N.S. (noam.sobel@weizmann.ac.il).

Received 10 March; accepted 4 August; published online 25 September 2011; doi:10.1038/nn.2926

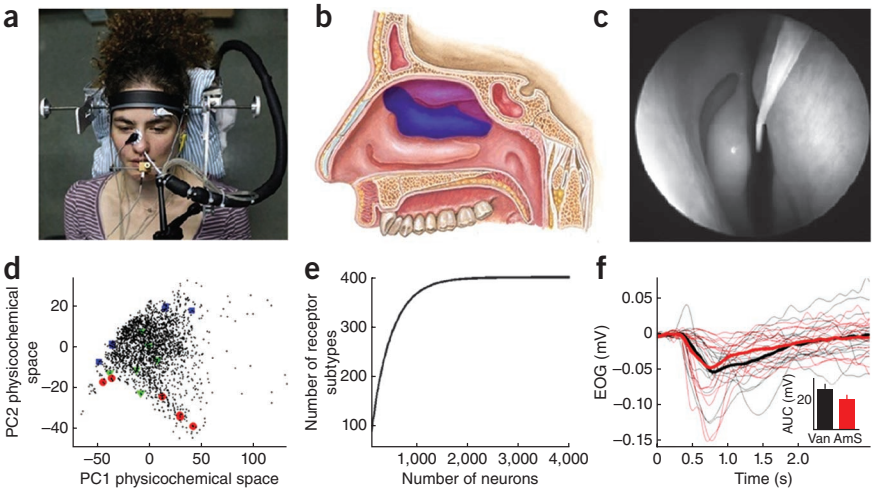

Figure 1 Experimental scheme. (**a**) Experimental setup. Subject was positioned in the non-invasive stereotactic device. The EOG electrode (fixed with holding bar in front of the nose) and heated olfactometer tube were inserted into the left nostril. EOG reference electrodes were placed on the nasal bone and left earlobe. Eye motion was recorded from above the left supraorbital area. (**b**) Sagittal section of the human nasal cavity, including the inferior, middle and superior turbinates. The approximate boundaries of the olfactory epithelium are marked in purple and the boundaries from which EOG recordings were obtained are overlaid in dark blue. (**c**) Endoscopic view of an EOG recording in a right nostril. On the right is the septum, and the shiny body is the middle turbinate, onto which the EOG electrode was nestled. (**d**) Three sets of six odorants spanning the first and second principal physicochemical axes. Black dots are 2,993 modeled odorants. Green triangles indicate the first set ($n = 12$), blue squares indicate the second set ($n = 16$) and red circles indicate the third set ($n = 13$). The odorants are plotted against a dataset of 2,993 odorants. For odorant specifications, see **Table 1**. (**e**) ORN collision count. Based on the birthday problem in probability theory, we calculated the expected number of different receptor subtypes expressed in increasing sample populations of ORNs given a random uniform distribution. At ~2,000 neurons, we reached the maximal number of different receptor subtypes with a probability of 95%. (**f**) Average EOGs from 16 subjects (thin lines), as well as grand average (thick lines) for the odorants vanillin (Van, black) and ammonium sulfide (AmS, red). Inlay is AUC and error bars represent within-subject sum of squares between conditions.

in odorant pleasantness; that is, a location that responded maximally to a pleasant odorant was likely to respond strongly to other pleasant odorants, and a location that responded maximally to an unpleasant odorant was likely to respond strongly to other unpleasant odorants. Finally, the extent of an individual's perceptual span predicted their span in evoked response; that is, individuals who perceived big differences across odorants also had big EOG differences across odorants. These results combined to suggest that, as with other distal senses, organization of the olfactory receptor surface in part reflects olfactory perception.

RESULTS

The statistics of the EOG response call for about five repetitions per odorant and a 45-s inter-stimulus interval[26,27]. A volunteer can rarely remain motionless in the non-invasive stereotactic device (**Fig. 1a**) for more than 2 h. Given that it takes up to an hour to place the apparatus in the nose and find a responsive location, we could only apply up to six different odorants in each experiment. We therefore used three batches of six odorants (**Table 1**), with each batch being applied to a separate group of, at minimum, 12 subjects, culminating in 18 odorants that spanned stimulus space (**Fig. 1d**). Overall, we obtained recordings in 57 of the 81 individuals that we studied, where we measured a response to 801 out of 1,974 odorant events (see Online Methods).

EOG tuning was recording site specific

Estimates of mammalian olfactory receptor neuron density vary between 8.3×10^4 and 3×10^5 per mm (refs. 2,6,28,29). Thus, an EOG likely reflects the summated generator potentials of anywhere between 2,000 and 35,000 neurons for an electrode of 117–350-μm diameter[6,11]. Our electrode had an inner diameter of 380 μm, putting it at the upper end of these estimations. Under the assumption of uniform and randomly distributed receptor subtypes, it is within 95% confidence that an EOG summating 2,000 neurons or more would contain all receptor subtypes (**Fig. 1e**). Thus, in an epithelium consisting of uniform and randomly distributed receptor subtypes, one would expect a similar EOG tuning profile no matter where the electrode was placed. With this in mind, we studied 16 subjects with a batch of six odorants (Experiment 1; **Fig. 2**). For each subject, we blindly placed the electrode and then cycled through the six odorants, delivering a single pulse of each. If any one of the odorants generated a response, we then commenced with the full experiment at that recording location. If none of the odorants generated a response, we shifted the electrode location and repeated the process[30].

Although uniform receptor subtype dispersion would predict that the greatest response would always be generated by the same odorant regardless of recording location, we instead observed a distribution of odorants that generated the maximal response. The number of times the maximal response was induced by odorants 1–6 was 3, 2, 3, 6, 3 and 1, respectively (**Fig. 2c**). The mean EOG area under the curve (AUC) induced by odorants 1–6 was -57.9 ± 6.5, -40.1 ± 5.1, -53.4 ± 3.9, -69.3 ± 7.9, -70.0 ± 7.4 and -42.6 ± 6.1 mV. Indeed, a two-way ANOVA interaction model revealed that the EOG tuning curve for these six odorants was not constant across subjects ($F_{75,132} = 2.39$, $P < 10^{-5}$). Moreover, a nonparametric approach revealed that the rank ordering of the EOG response was not correlated across subjects (Kruskal-Wallis, $H_5 = 9$, $P = 0.11$). This result is inconsistent with the notion of a random and uniform distribution of receptor subtypes and suggests that, for each location, there was a subset of receptors that best responded to one of the six odorants.

One may raise the possibility that these differences did not reflect a difference across recording locations, but rather a difference across subjects[31,32], and that, had we recorded from different locations in the same subject, we would always get the same response. To address this, we repeated the experiment in a single subject three times, searching for a responsive location once only with odorant 1, once only with odorant 3 and once only with odorant 5 (Experiment 2). Again, in contrast with the expectation generated by a random and uniform distribution of receptor subtypes, we observed an independent location that was maximally tuned to each of the three odorants that we used to identify a responsive location (**Fig. 2d–f**). An ANOVA revealed that these tuning curves differed

Table 1 The odorants used, their dilution and perception

Index	CID	CAS	Name	Pleasantness	Intensity	PC1	PC2	DilOil	DilAir
Set 1									
1	176	64-19-7	Acetic acid	0.41 ± 0.06	1.86 ± 0.39	–48.7	–7.3	0.1% PEG	100%
2	612	50-21-5/598-82-3	Lactic acid	0.24 ± 0.05	2.06 ± 0.40	–36.6	1.7	20% PEG	100%
3	650	431-03-8	2,3-butanedione	0.52 ± 0.10	2.44 ± 0.42	–36.2	0.6	0.02% PEG	100%
4	6501	77-83-8	Ethyl 3-methyl-3phenylglycidate	0.59 ± 0.11	2.31 ± 0.41	14.1	18.8	10% MO	50%
5	93009	5655-61-8	Bornyl acetate	0.51 ± 0.10	2.56 ± 0.33	15. 3	19.8	1% PEG	100%
6	91497	1222-05-5/keine	1,3,4,6,7,8-Hexahydro-4,6,6, 7,8,8-hexamethylcyclopenta[g]-2-benzopyran in 50% DEP	0.38 ± 0.08	2.28 ± 0.38	39.8	17. 8	20% MO	100%
Set 2									
1	261	123-72-8	Butyraldehyde	0.53 ± 0.08	0.91 ± 0.28	–38.6	–12.7	0.01% PEG	43%
2	7888	107-75-5	Hydroxycitronellal	0.48 ± 0.08	1.61 ± 0.31	6.5	–6.3	30% PEG	25%
3	12348	628-63-7	Amyl acetate	0.88 ± 0.07	1.59 ± 0.31	–12.9	–11.2	0.3% PEG	22%
4	8797	140-39-6	p-Cresyl acetate	0.78 ± 0.09	1.67 ± 0.26	–7.6	7.5	0.7% PEG	23%
5	643820	106-25-2	Nerol	0.13 ± 0.05	1.75 ± 0.30	–1.2	0.4	50% PEG	22%
6	957	111-87-5	Octanol	0.54 ± 0.12	1.72 ± 0.31	–9.0	–22.5	13% PEG	33%
Set 3									
1	1031	71-23-8	1-Propanol	0.42 ± 0.12	1.35 ± 0.20	–45.1	–17.3	100%	10%
2	9609	352-93-2	Diethyl sulfide	0.32 ± 0.10	0.86 ± 0.18	–36.9	–15	0.01% PEG	12%
3	8918	143-13-5	Nonyl acetate	0.73 ± 0.07	1.38 ± 0.17	11.6	–24.1	100%	30%
4	14228	1117-55-1	Hexyl octanoate	0.53 ± 0.09	0.88 ± 0.16	28.5	–33.3	100%	30%
5	7800	106-33-2	Ethyllaurat	0.55 ± 0.10	1.28 ± 0.20	28.7	–34.1	100%	100%
6	31283	124-06-1	Ethyl myristate	0.57 ± 0.11	1.12 ± 0.19	40.85	–38.7	100%	60%

Regarding reported pleasantness and intensity, note that the critical values for the analyses were not the cross-subject means reported here, but rather the within-subject means, as this study revolves around within-subjects comparisons between EOG and perception. CID, compound identification number; DilAir, dilution with clean air using the olfactometer; DilOil, dilution with oil in liquid phase; MO, mineral oil; PC1, principal component 1; PC2, principal component 2; PEG, propylene glycol.

significantly ($F_{10,16} = 28.5$, $P < 10^{-7}$). Moreover, a nonparametric approach revealed that the rank ordering of the EOG response was not correlated across locations (Kruskal-Wallis, $H_5 = 3.5$, $P = 0.62$). In other words, the EOG tuning was recording site specific.

These results suggest that a given patch of epithelium, as defined by the responsive area under the EOG electrode, has a unique functional response pattern. Given such a patched epithelium, one would predict that, had we used only one odorant to identify recording cites, we would then obtain a similar response profile across subjects. To test this, we used only one of a new batch of six odorants (odorant 4, p-cresyl acetate, Chemical Abstract Services (CAS) no. 140-39-6) to search for a responsive site and then measured the response to all six odorants at that location (Experiment 3). Consistent with the notion of patchy epithelium, odorant 4 induced the maximal response in 10 of the 12 subjects in which it was used to identify a responsive location (**Fig. 3**). Here, odorant 4 stood out for its selectivity, not for its response magnitude, which was similar to that of strong responses in the first two experiments (**Fig. 3**). The mean EOG AUC induced by odorants 1–6 was 0.4 ± 1.8, –4.3 ± 1.9, –2.6 ± 2.7, –53.9 ± 7.6, –7.2 ± 7.6 and –7.8 ± 1.7 mV. Consistent with our prediction, a two-way ANOVA interaction model revealed that the odorant response distribution was not significantly different across subjects ($F_{55,70} = 0.78$, $P = 0.82$). Moreover, a nonparametric approach revealed that the rank ordering of the EOG response was indeed correlated across subjects (Kruskal-Wallis, $H_5 = 12.65$, $P < 0.03$).

Using a particular odorant from the set to search for a responsive location entailed extensive exposure to that odorant, and this may have somehow influenced the response. With this in mind, we first used an independent odorant (L-carvone, CAS no. 6485-40-1) to identify a responsive site and then tested a new batch of six odorants at that site (Experiment 4). This yielded a bimodal response profile. Subjects 1–6 responded maximally to different odorants,

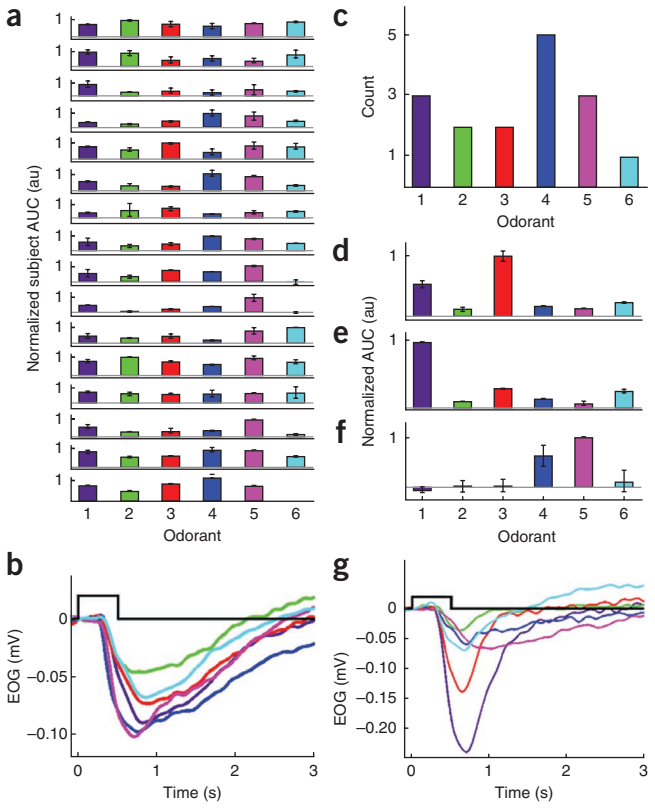

Figure 2 Different localizer odorants revealed different epithelial response profiles. (**a**–**c**) Experiment 1. (**a**) Each subject's normalized AUC. Odorants are color-coded and numbered according to set 1 of **Table 1**. (**b**) Grand averaged EOG responses ($n = 16$, stimulus duration = 500 ms). Black square-wave reflects odorant onset/offset. (**c**) Number of times each of the six odorants elicited the maximal EOG AUC. (**d**–**g**) Experiment 2. (**d**) Subject-normalized AUC with odorant 3 as localizer. (**e**) Subject-normalized AUC with odorant 1 as localizer. (**f**) Subject normalized AUC with odorant 5 as localizer. (**g**) Averaged EOGs obtained in three recording sessions (**d**–**f**) from different locations in a single subject. Black square-wave reflects odorant onset/offset. Error bars are s.e.m., au are arbitrary units.

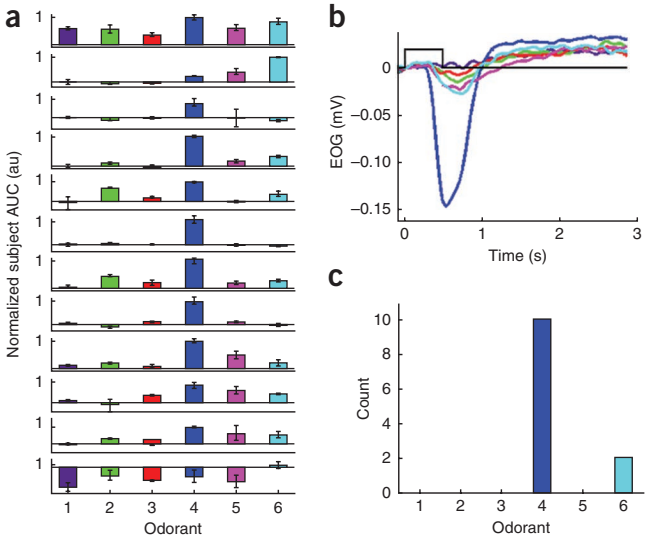

Figure 3 A common localizer odorant revealed common epithelial response profiles. (**a**) Experiment 3, each subject's normalized AUC. Odorants are color coded, and numbered according to set 2 of **Table 1**. (**b**) Grand averaged EOG responses ($n = 12$, stimulus duration = 500 ms). Black square-wave reflects odorant onset/offset. (**c**) Number of times each of the six odorants elicited the maximal EOG AUC. In 10 of 12 subjects, the maximal response was for the odorant used to localize the recording site. Error bars are s.e.m., au are arbitrary units.

mostly odorant 1. Subjects 7–15 all responded maximally to odorant 5 (**Fig. 4**). The mean EOG AUC induced by odorants 1–6 was −45.4 ± 4.5, −40.3 ± 2.6, −33.4 ± 2.9, −19.1 ± 1.8, −41.7 ± 3.8 and −31.7 ± 5.7 mV. Overall, this amounted to a variable response profile ($F_{60,75} = 5.95$, $P < 10^{-12}$). Moreover, a nonparametric approach revealed that the rank ordering of the EOG response was indeed correlated across subjects (Kruskal-Wallis, $H_5 = 13.96$, $P < 0.02$).

The bimodal profile may reflect one of two possibilities. In that subject numbering reflects their chronological order in time, examination of the data suggests that, from the seventh subject onward, the response pattern apparently changed (**Fig. 4a**). Thus, one possibility is that an independent factor that we failed to identify influenced the result. Alternatively, it remains possible that the localizer odorant indeed activated areas that were responsive to both odorants 1 and 5. These alternative interpretations, however, do not substantially influence the main implications of this data (see Discussion).

Finally, despite a psychophysical test that implied non-trigeminality of the low odorant concentrations that we used (see Online Methods), we set out to conduct a final test using pure olfactants to insure that the EOGs can be obtained from non-trigeminal sources. We recorded from 16 subjects in which we searched for a responsive location using the pleasant pure olfactory odorant vanillin[33] (Experiment 5). After identifying a responsive location, we commenced with the experiment using both vanillin and the unpleasant odorant ammonium sulfide, which we have found to be non-trigeminal at low concentrations. We measured a clear response to both odorants, validating the olfactory source of EOGs (**Fig. 1f**). Moreover, consistent with the previous experiments, vanillin and ammonium sulfide generated a significantly different response (binomial, $P < 0.04$), with an AUC greater for vanillin in 12 subjects and greater for ammonium sulfide in four subjects.

To summarize these results, if the epithelium consisted of uniform and randomly distributed receptor subtypes, then our results would be unlikely. One could not expect such specificity of site given random and uniform receptor subtype distribution. Thus, consistent with previous studies[9–12,14,34], our results imply that olfactory receptor subtypes are not uniformly and randomly distributed, but are rather concentrated in patches on the olfactory epithelium.

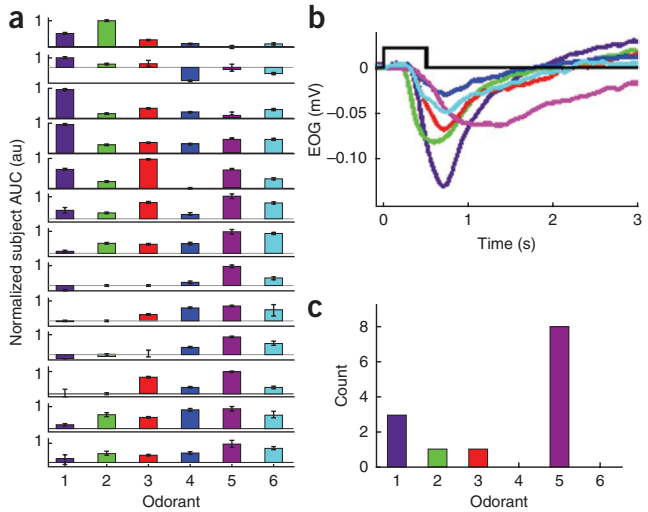

Figure 4 An external common localizer odorant revealed a bimodal epithelial response profile. Experiment 4: EOG recordings conducted after searching for responsive locations with L-carvone. (**a**) Each subject's normalized AUC. Odorants are color coded, and numbered according to set 3 of **Table 1**. (**b**) Grand averaged EOG responses ($n = 13$, stimulus duration = 500 ms). Black square-wave reflects odorant onset/offset. (**c**) Number of times each of the six odorants elicited the maximal EOG AUC. Error bars are s.e.m., au are arbitrary units.

Inherent, rather than imposed, response patterns

The EOG may be influenced by imposed, rather than inherent, epithelial properties, and the patchy response profile may not necessarily reflect receptor subtype distribution. Imposed patterns reflect a combination of sniff-related flow properties and odorant sorption properties[35–37]. Here, subjects did not sniff, and odorants were introduced at a constant flow. Thus, the remaining potentially imposed component relates to odorant sorption.

To address the possible influence of sorption properties, we used previously collected data[15] to generate a simple optimized physicochemical metric that reflects epithelial sorption (see Online Methods). Odorant pairwise distance in this physicochemical sorption metric significantly correlated with odorant pairwise difference in retention time across bullfrog mucosa[15] ($r = 0.78$, $P < 10^{-10}$ for log(retention time) values; **Fig. 5a**). We did not find a relation between odorant pairwise distances in this physicochemical sorption metric and our measured odorant pairwise distances in EOG AUC ($r = 0.13$, $P = 0.06$; **Fig. 5b**). In other words, the imposed properties that follow odorant sorption alone could not explain our results, which likely reflect, in part, inherent patterns related to olfactory receptor subtype distribution.

The EOG is tuned to olfactory perception

Assuming an inherently driven response profile, we next set out to ask what axis governs this response organization. We tested alternative tuning axes, some related to perception and others related to odorant structure. For each dataset, we calculated the distance in EOG responses and then tested for a relation between these response distances and their respective odorants' distances in perceptual (pleasantness, intensity and trigeminality) and physicochemical spaces. Briefly, to calculate EOG distance, per subject, we represented each odorant's

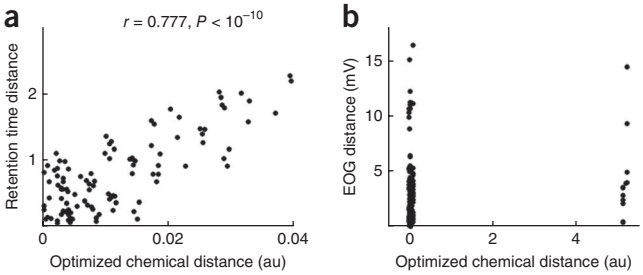

Figure 5 EOGs were unrelated to odorant sorption. (**a**) Relation between the optimized sorption metric (see Online Methods) and the actual mucosal retention times reported in the bullfrog[15]. Each point is a pairwise odorant comparison. (**b**) Relation between this same optimized sorption metric and EOG distances measured here. Each point is the mean odorant pairwise distance per odorant pair per subject; that is, points = $n \times 5$. No relation is evident. Note, however, that the model is bound by the limited physicochemical span of the bullfrog experiment odorant selection, as evident in the restricted *x*-axis span in **a**. au are arbitrary units.

average EOG as a vector and calculated the Euclidean distance between these vectors (see Online Methods). To calculate perceptual distance per subject, we measured the normalized distance between odorant scores provided by the subject on visual-analog scales. To calculate physicochemical distances, we used the Euclidean distance between odorants represented by 1,491 physicochemical descriptors[38]. For these analyses, we only considered subjects who responded to at least three of the odorants used, to allow for a meaningful correlation analyses (this eliminated nine subjects, retaining 32).

The distance in odorant perceived pleasantness was significantly correlated with distance in odorant-induced EOG ($r = 0.42$, $P < 10^{-7}$; after retaining all 41 subjects in the analysis, this correlation grows to $r = 0.45$, $P < 10^{-10}$; **Fig. 6a**). In other words, a location that responded maximally to a pleasant odorant was more likely to respond strongly to other pleasant odorants, and a location that responded maximally to an unpleasant odorant was more likely to respond strongly to other unpleasant odorants. In contrast, the pairwise distances in odorant perceived intensity was unrelated to the odorant pairwise EOG distance ($r = 0.09$, $P < 0.26$), and pairwise distance in odorant trigeminality showed a statistically significant, but weak, correlation to the odorant pairwise EOG distance ($r = 0.23$, $P < 0.01$), a correlation that was significantly weaker than with pleasantness (difference between normalized correlations, $Z = 1.89$, $P = 0.028$).

The correlation between distances in odorant pleasantness and distances in EOG response may be, in part, artificially imposed by the structure of the data combined with measurements of distances rather than vectors. To address this, we randomly reassigned the odorant pleasantness ratings and recalculated the correlationr r100 times. The average correlation of the shuffled values was $\langle r \rangle = 0.21 \pm 0.003$ ($\langle P \rangle = 0.05$). This correlation was significantly lower than that obtained for the unscrambled data (difference between normalized correlations, $Z = 2.04$, $P = 0.02$). In other words, the relation of EOG to pleasantness was significantly stronger than would be expected by chance.

After establishing a link between EOG and an axis of odorant perception, we set out to investigate links between EOG and axes of odorant structure. The pairwise odorant distance in physicochemical space, as defined by the Euclidean distance in a 1,491 descriptor space[38], was also a significant predictor of the pairwise EOG distance ($r = 0.24$, $P < 0.002$; **Fig. 6b**), yet this correlation was significantly weaker than that with pleasantness (difference between normalized correlations, $Z = 1.82$, $P = 0.03$). Substituting the Euclidean physicochemical metric with PC1 of physicochemical space[19] yielded a similar correlation ($r = 0.22$, $P = 0.005$), which was also significantly weaker than the correlation of EOG distance with pleasantness (difference between normalized correlations, $Z = 1.95$, $P = 0.026$). Moreover, substituting the Euclidean physicochemical metric with a rodent-data optimized set of physicochemical descriptors[38] yielded a null result ($r = 0.14$, $P = 0.08$).

Finally, we asked whether any individual physicochemical descriptor alone could predict EOG response. Only 184 of the 1,491 descriptors generated a normal distribution of values for the 18 odorants in question, thus allowing a correlational analysis. Of these, none of the descriptors were significantly correlated with EOG distance (best correlation was for the descriptor R6e+, $r = 0.10$, $P = 0.12$).

Perceptual span predicted EOG span

Despite our testing of various alternative axes, odorant pleasantness remained the best predictor of EOG. That said, the weak, yet disturbing, correlation that nevertheless emerged between shuffled pleasantness ratings and the EOG response ($\langle r \rangle = 0.21$, $\langle P \rangle = 0.05$) drove us to further investigate the relation between EOG and perception. We asked whether subjects who had a large span in their perception also had a large span in their EOG. The span is the distance between the smallest and largest measurement obtained in a subject. This analysis revealed a correlation of $r = 0.497$, $P < 0.002$ (**Fig. 6c**). In other words, individuals who perceived big differences across odorants also had big EOG differences across odorants. Critically, randomly shuffling pleasantness span values 100 times revealed no meaningful correlation ($\langle r \rangle = -0.004$, $\langle P \rangle = 0.46$), and physichochemical span was unrelated to EOG span ($r = -0.01$, $P = 0.95$). In other words, properties of the EOG were clearly linked to perception.

Finally, to estimate the influence of subjects with reduced EOG span on the overall relation of EOG to pleasantness, we conducted a median

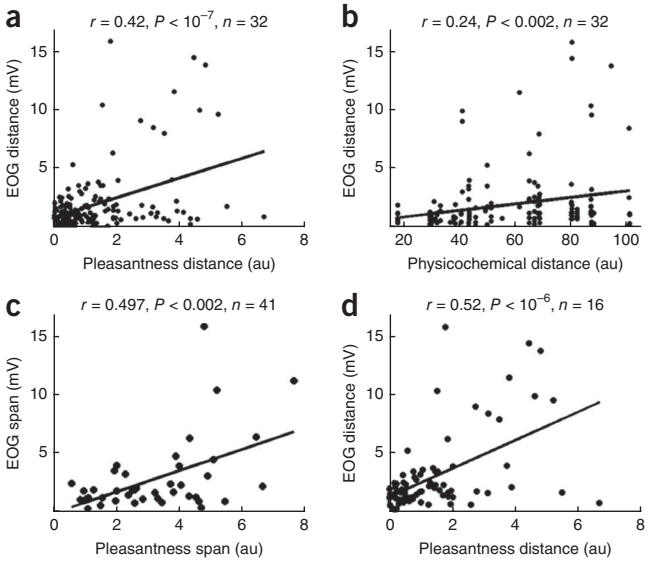

Figure 6 EOGs were tuned to olfactory perception. In **a**, **b** and **d**, each point is the mean odorant pairwise distance per odorant pair per subject; that is, points = $n \times 5$. In **c**, each point is a subject. (**a**) Correlation between pleasantness distances and EOG distances ($n = 32$). (**b**) Correlation between chemical Euclidean distance and EOG distance ($n = 32$). (**c**) Correlation between pleasantness span and EOG span ($n = 41$). (**d**) Correlation between EOG distance and pleasantness distance for the subjects with largest EOG span ($n = 16$). au are arbitrary units.

split of subjects according to their EOG span and recalculated the correlation between EOG and pleasantness in the remaining 16 subjects. Note that this is not a split according to the power of the correlation, but rather only according to the extent of the EOG span; that is, we retained subjects who provided more information that could either favor or decrease the correlation. Following this split, the correlation increased from $r = 0.42$ ($P < 10^{-7}$) to $r = 0.52$ ($P < 10^{-6}$) (**Fig. 6d**).

DISCUSSION

Consistent with previous studies that characterized the functional response properties of the olfactory epithelium, we observed a patchy receptive surface. When we probed the epithelium using different odorants, we found maximally responsive regions for each. When we probed the epithelium using one odorant, we found an area maximally responsive to that odorant in most subjects. The possibility that this response topography exclusively reflected imposed patterns of response is minimal in light of the lack of correlation between the response and a physicochemical estimate of sorption. Taken together, if receptor subtype identity indeed governs EOG response profile, then receptor subtypes were not randomly and uniformly distributed.

Although this patchy response profile echoes numerous other studies[9–14], here we were also able to plot this response pattern as a function of human perception. This revealed a modest, but clear, and highly significant correlation between the response pattern and the perception of odorant pleasantness. In other words, as in vision and audition, organization of the receptor surface in olfaction reflects a primary perceptual axis.

One may ask how these results would transfer to the real world, where, unlike the monomolecular odorants that we tested, odor objects are often made of hundreds of different molecules. In considering this, it is important to remember that, although natural odor objects may contain hundreds of different molecules, their constituents are not present with equal magnitude. For example, natural rose may have 172 volatile monomolecules, but 70% of its headspace consists of only one molecule, PEA[39]. Thus, the rose-induced epithelial pattern would be dominated by patches responsive to PEA. The remaining activated locations may then contribute to the overall image by some average or additive representation.

Although our results imply a hard-wired aspect of odorant pleasantness, they do not imply that odorant pleasantness is unmalleable, as a portion of perception that is hardwired at the receptive surface does not rule out later remapping. This is clearly evidenced in vision[40]. For example, location in the world is hardwired to location on the retina. Nevertheless, context and experience can shift spatial perception (for example, Muller-Lyer illusion)[41]. Similarly, perceived color is hardwired to wavelength. Nevertheless, the same wavelength can be perceived as an entirely different color as a function of the context in which it is viewed[40]. Here we suggest that odorant pleasantness is mapped onto the olfactory epithelium, yet this mapping is malleable by context and experience, which influence possibly epithelial, and without question later processing stages[42–44].

Our key finding was that activity patterns at the epithelium correlated with odorant perception. We also found that these activity patterns correlated weakly with various physicochemical axes. In turn, functional magnetic resonance imaging data has revealed a physicochemical-based representation in the anterior piriform cortex[45]. Because such a representation in piriform would be dependent on maintenance of this information in epithelium and bulb, these findings can be construed as disagreeing. However, our finding of epithelial neural activity that better correlated with a perceptual, rather than a structural, axis does not infer that the latter doesn't exist. In other words, the fact that a key perceptual axis is reflected in olfactory epithelium does not prevent the epithelium from conveying information on structure. Thus, we stress that our most important finding is the correlation that we uncovered, rather than those that we did not.

Although it is tempting to relate interchangeably between previous results from rodents and our results, this must be done with caution. The cellular organization of human olfactory epithelium may be more patchy than rodent epithelium[46]. Moreover, organizational principals may differ throughout the olfactory pathway, as humans have a substantially larger number of bulbar glomeruli than are predicted from rodent organizational principals[47]. Thus, our results pertain to organization of the human olfactory system. This, of course, is not a drawback, but rather something to keep in mind when relating our findings to the bulk of the literature.

Our study has several inherent caveats. First, olfactory perception depends on sniffing[48,49]. Sniffs, however, contaminate the EOG and were therefore prevented. Although odorant pleasantness perception with and without sniffing was correlated ($r = 0.65$, $P < 10^{-7}$, see Online Methods), percepts with and without sniffing were not identical. Second, although human olfactory epithelium likely extends into cribriform plate[46], subject safety considerations limited our recordings to the medial turbinate. Third, we cannot make definitive claims as to the overall size of a functional patch or to the full range of patch odorant specificity. Finally, the experiment duration restriction, combined with the need for repeated trials, minimized the flexibility in experimental design. Indeed, these inherent caveats may underlie the apparent shift in response profile starting with subject 7 in the fourth experiment. This shift, however, did not introduce a result, but rather weakened our main result, as it reduced the correlation between EOG response distance and odorant pleasantness distance.

Despite these inherent weaknesses, the unique opportunity of collecting perceptual data from the same subjects in which we recorded neural activity allowed us to uncover an organizational feature of the human olfactory epithelium. Specifically, we conclude that the organization of the human olfactory epithelium reflects, in part, an important axis of human olfactory perception, namely odorant pleasantness.

METHODS

Methods and any associated references are available in the online version of the paper at http://www.nature.com/natureneuroscience/.

Note: Supplementary information is available on the Nature Neuroscience website.

ACKNOWLEDGMENTS

This work was supported by ERC-FP7 Ideas grant #200850 and by the James S. McDonnell Foundation.

AUTHOR CONTRIBUTIONS

H.L. and N.S. conceived the study. H.L., S.S., A.P., T.H., Y.R. and N.S. designed the experiments. H.L., S.S. and A.P. performed the experiments. H.L., E.S., H.V. and N.S. analyzed the data. H.L., T.H., E.S. and N.S. wrote the manuscript.

COMPETING FINANCIAL INTERESTS

The authors declare no competing financial interests.

Published online at http://www.nature.com/natureneuroscience/.
Reprints and permissions information is available online at http://www.nature.com/reprints/index.html.

1. DeValois, R.L. & DeValois, K.K. Spatial vision. in *Encyclopedia of the Human Brain* (ed. Ramachandran, V.S.) 419–431 (Academic Press, New York, 2002).
2. Vater, M. & Kossl, M. Comparative aspects of cochlear functional organization in mammals. *Hear. Res.* **273**, 89–99 (2010).
3. Fleischer, J., Breer, H. & Strotmann, J. Mammalian olfactory receptors. *Front. Cell. Neurosci.* **3**, 9 (2009).

4. Iwema, C.L., Fang, H., Kurtz, D.B., Youngentob, S.L. & Schwob, J.E. Odorant receptor expression patterns are restored in lesion-recovered rat olfactory epithelium. *J. Neurosci.* **24**, 356–369 (2004).
5. Miyamichi, K., Serizawa, S., Kimura, H.M. & Sakano, H. Continuous and overlapping expression domains of odorant receptor genes in the olfactory epithelium determine the dorsal/ventral positioning of glomeruli in the olfactory bulb. *J. Neurosci.* **25**, 3586–3592 (2005).
6. Moran, D.T., Rowley, J.C. III, Jafek, B.W. & Lovell, M.A. The fine structure of the olfactory mucosa in man. *J. Neurocytol.* **11**, 721–746 (1982).
7. Gilad, Y., Bustamante, C.D., Lancet, D. & Paabo, S. Natural selection on the olfactory receptor gene family in humans and chimpanzees. *Am. J. Hum. Genet.* **73**, 489–501 (2003).
8. Kauer, J.S. & Moulton, D.G. Responses of olfactory bulb neurones to odor stimulation of small nasal areas in the salamander. *J. Physiol. (Lond.)* **243**, 717–737 (1974).
9. Edwards, D.A., Mather, R.A. & Dodd, G.H. Spatial variation in response to odorants on the rat olfactory epithelium. *Experientia* **44**, 208–211 (1988).
10. Ezeh, P.I., Davis, L.M. & Scott, J.W. Regional distribution of rat electroolfactogram. *J. Neurophysiol.* **73**, 2207–2220 (1995).
11. Mackay-Sim, A. & Kesteven, S. Topographic patterns of responsiveness to odorants in the rat olfactory epithelium. *J. Neurophysiol.* **71**, 150–160 (1994).
12. Scott, J.W., Shannon, D.E., Charpentier, J., Davis, L.M. & Kaplan, C. Spatially organized response zones in rat olfactory epithelium. *J. Neurophysiol.* **77**, 1950–1962 (1997).
13. Leopold, D.A. *et al.* Anterior distribution of human olfactory epithelium. *Laryngoscope* **110**, 417–421 (2000).
14. Kent, P.F., Mozell, M.M., Youngentob, S.L. & Yurco, P. Mucosal activity patterns as a basis for olfactory discrimination: comparing behavior and optical recordings. *Brain Res.* **981**, 1–11 (2003).
15. Mozell, M.M. & Jagodowicz, M. Chromatographic separation of odorants by the nose: retention times measured across *in vivo* olfactory mucosa. *Science* **181**, 1247–1249 (1973).
16. Hornung, D.E. & Mozell, M.M. Odorant removal from the frog olfactory mucosa. *Brain Res.* **128**, 158–163 (1977).
17. Schiffman, S.S. Physicochemical correlates of olfactory quality. *Science* **185**, 112–117 (1974).
18. Richardson, J.T. & Zucco, G.M. Cognition and olfaction: a review. *Psychol. Bull.* **105**, 352–360 (1989).
19. Khan, R.M. *et al.* Predicting odor pleasantness from odorant structure: pleasantness as a reflection of the physical world. *J. Neurosci.* **27**, 10015–10023 (2007).
20. Zarzo, M. Psychologic dimensions in the perception of everyday odors: pleasantness and edibility. *J. Sens. Stud.* **23**, 354–376 (2008).
21. Yeshurun, Y. & Sobel, N. An odor is not worth a thousand words: from multidimensional odors to unidimensional odor objects. *Annu. Rev. Psychol.* **61**, 219–241 (2010).
22. Saito, H., Chi, Q., Zhuang, H., Matsunami, H. & Mainland, J.D. Odor coding by a mammalian receptor repertoire. *Sci. Signal.* **2**, 9 (2009).
23. Haddad, R. *et al.* Global features of neural activity in the olfactory system form a parallel code that predicts olfactory behavior and perception. *J. Neurosci.* **30**, 9017–9026 (2010).
24. Keller, A., Zhuang, H., Chi, Q., Vosshall, L.B. & Matsunami, H. Genetic variation in a human odorant receptor alters odor perception. *Nature* **449**, 468–472 (2007).
25. Garcia, G.J., Tewksbury, E.W., Wong, B.A. & Kimbell, J.S. Interindividual variability in nasal filtration as a function of nasal cavity geometry. *J. Aerosol Med. Pulm. Drug Deliv.* **22**, 139–155 (2009).
26. Kobal, G. *Elektrophysiologische Untersuchungen des menschlichen Geruchssinns.* (Thieme Verlag, Stuttgart, 1981).
27. Lapid, H. *et al.* Odorant concentration dependence in electroolfactograms recorded from the human olfactory epithelium. *J. Neurophysiol.* **102**, 2121–2130 (2009).
28. Mackay-Sim, A. & Kittel, P. Cell dynamics in the adult mouse olfactory epithelium: a quantitative autoradiographic study. *J. Neurosci.* **11**, 979–984 (1991).
29. Menco, B.P. Qualitative and quantitative freeze-fracture studies on olfactory and nasal respiratory structures of frog, ox, rat and dog. I. A general survey. *Cell Tissue Res.* **207**, 183–209 (1980).
30. Knecht, M. & Hummel, T. Recording of the human electro-olfactogram. *Physiol. Behav.* **83**, 13–19 (2004).
31. Hasin-Brumshtein, Y., Lancet, D. & Olender, T. Human olfaction: from genomic variation to phenotypic diversity. *Trends Genet.* **25**, 178–184 (2009).
32. Keller, A. & Vosshall, L.B. Influence of odorant receptor repertoire on odor perception in humans and fruit flies. *Proc. Natl. Acad. Sci. USA* **104**, 5614 (2007).
33. Doty, R.L. *et al.* Intranasal trigeminal stimulation from odorous volatiles: psychometric responses from anosmic and normal humans. *Physiol. Behav.* **20**, 175–185 (1978).
34. Sakano, H. Neural map formation in the mouse olfactory system. *Neuron* **67**, 530–542 (2010).
35. Wise, P.M., Zhao, K. & Wysocki, C.J. Dynamics of nasal chemesthesis. *Ann. NY Acad. Sci.* **1170**, 206–214 (2009).
36. Yang, G.C., Scherer, P.W. & Mozell, M.M. Modeling inspiratory and expiratory steady-state velocity fields in the Sprague-Dawley rat nasal cavity. *Chem. Senses* **32**, 215–223 (2007).
37. Scott, J.W., Acevedo, H.P., Sherrill, L. & Phan, M. Responses of the rat olfactory epithelium to retronasal air flow. *J. Neurophysiol.* **97**, 1941–1950 (2007).
38. Haddad, R. *et al.* A metric for odorant comparison. *Nat. Methods* **5**, 425–429 (2008).
39. Ayci, F., Aydinli, M., Bozdemir, Ö.A. & Tutaş, M. Gas chromatographic investigation of rose concrete, absolute and solid residue. *Flavour Fragrance J.* **20**, 481–486 (2005).
40. Purves, D., Beau Lotto, R., Mark Williams, S., Nundy, S. & Yang, Z. Why we see things the way we do: evidence for a wholly empirical strategy of vision. *Phil. Trans. R. Soc. Lond. B* **356**, 285 (2001).
41. Howe, C.Q. & Purves, D. The Müller-Lyer illusion explained by the statistics of image-source relationships. *Proc. Natl. Acad. Sci. USA* **102**, 1234 (2005).
42. Wesson, D.W. & Wilson, D.A. Sniffing out the contributions of the olfactory tubercle to the sense of smell: hedonics, sensory integration, and more? *Neurosci. Biobehav. Rev.* **35**, 655–668 (2011).
43. Li, W. *et al.* Right orbitofrontal cortex mediates conscious olfactory perception. *Psychol. Sci.* **21**, 1454–1463 (2010).
44. Gottfried, J.A. & Dolan, R.J. The nose smells what the eye sees: crossmodal visual facilitation of human olfactory perception. *Neuron* **39**, 375–386 (2003).
45. Gottfried, J.A., Winston, J.S. & Dolan, R.J. Dissociable codes of odor quality and odorant structure in human piriform cortex. *Neuron* **49**, 467–479 (2006).
46. Moran, D.T. Anatomy and ultrastructure of the human olfactory neuroepithelium. in *Handbook of Olfaction and Gustation* (ed. Doty, R.L.) 75–102 (Marcel-Dekker, New York, 1995).
47. Maresh, A., Rodriguez Gil, D., Whitman, M.C. & Greer, C.A. Principles of glomerular organization in the human olfactory bulb—implications for odor processing. *PLoS ONE* **3**, e2640 (2008).
48. Kepecs, A., Uchida, N. & Mainen, Z.F. The sniff as a unit of olfactory processing. *Chem. Senses* **31**, 167–179 (2006).
49. Mainland, J. & Sobel, N. The sniff is part of the olfactory percept. *Chem. Senses* **31**, 181–196 (2006).

ONLINE METHODS

Subjects. Recording EOGs was attempted in 81 normosmic healthy subjects. The experiment concluded prematurely in 24 subjects, primarily as a result of movement of the recording electrode. Thus, data from 57 subjects (37 women, mean age = 26.8 years) who completed the experiment were submitted to further analysis. All subjects provided written informed consent to procedures approved by the Helsinki Committee. Subjects had no history of neurological, sinus or nasal disease.

Odorant selection. First, we generated a physicochemical odorant space containing 2,993 molecules. To this end, we downloaded the odorant's three-dimensional molecular structure files from PubChem (http://pubchem.ncbi.nlm.nih.gov/), used analytical chemistry software (Dragon Talete, http://www.talete.mi.it/index.htm) to obtain 1,491 chemical descriptors for each odorant and used principal component analysis to replot the odorants in a two-dimensional space made of the first and second principal components (PC1 and PC2). We then selected odorant sets 1 and 3 such that they spanned PC1 and had either upper (set 1) or lower (set 3; **Fig. 1d**) boundary projections on PC2. These sets contained pairs of odorants that were chemically close. Odorant set 2 was chosen such that it contained three pairs of odorants that each had a similar functional group, but differed in percept (**Fig. 1d**, aldehydes, alcohols and esters in **Table 1**).

Odorant dilution. In each experiment, odorants were first diluted in either propylene glycol (PEG, 57-55-6) or mineral oil (8042-47-5) to equate expected intensity according to the odorant's vapor pressure. To further equate the perceived intensities, we then individually diluted odorants with clean, heated and humidified air using a fully automated olfactometer, such that they were rated as equally intense (within two s.d.) by an independent group of seven subjects. Odorant delivery parameters during intensity equation were identical to those later used in the EOG recordings.

Stimulus delivery and experiment design. For odorant stimulation, a computer-controlled 30-channel air-dilution olfactometer was used. This olfactometer delivered odorants into the recorded nostril via Teflon tubing (inner diameter = 2.15 mm), maintaining steady mechanical and thermal conditions (constant flow of 5.5 l min^{-1}, temperature of 37 °C and relative humidity of 80%). Stimulus duration was 500 ms, and inter-stimulus-interval was 45 s. In a given experiment, a minimum of four repetitions for each of the six odorants was presented in a fully randomized manner, followed by four clean air, or blank, events. To avoid mucosal sniff artifacts, a digitized voice asked subjects to hold their breath for 1.5 s before stimulation onset and 3 s thereafter. Following the recording epoch, subjects ranked the intensity and pleasantness of the stimulus on separate visual-analog scales.

Recording apparatus. We have previously described EOG recording in detail[27]. Here, we also used an improved non-invasive stereotactic head holder (**Fig. 1a**). We recorded olfactory EOG, visual EOG, electrocardiogram and nasal airflow by spirometer, all at 1 kHz, with a 50-Hz notch filter to exclude electrical-system noise.

Preprocessing EOG responses. False-negative EOG recordings were abundant. In such cases there was no evident EOG response despite a clear percept. Such false negatives can occur for various reasons, primarily micro-movement of the electrode during the experiment. To control for these cases, we built a Matlab-based graphical user interface (Matlab R2009b, The MathWorks) that simultaneously presented all repeated measures of EOGs, eye movements, respiration and heartbeats to a single odorant in one experiment session (4–5 repeats). We then selected only successful repetitive recordings, omitting respiratory artifacts, eye-blinks, abrupt facial movements and sudden flat responses, culminating in 801 successful recordings out of 1,974 odor events. Baseline was corrected in each recording by subtraction of the mean value during the first 150 ms from stimulus onset. That is, all responses were now aligned to $V = 0$ at $t = 0$ (response onset (t rise) was typically equal to or larger than 150 ms; **Supplementary Fig. 1**). We low-passed filtered the data to include frequencies lower or equal to 5 Hz and then calculated the subject averaged responses.

EOG distances. To calculate the EOG distance within subject, we first extracted the amplitudes and latencies of the mean responses of each subject. To calculate the response's AUC, we defined a time window for integration according to the odorant that evoked the maximal amplitude. The time window for integration was from 100 ms before $1/e$ of the response amplitude, and up to 100 ms after recurrence to 90% of the response amplitude (**Supplementary Fig. 1**). This time window provided maximal signal to noise ratio across all data collected. For correlation analysis between EOG distances and other measures, we defined an exclusion criterion by which subjects with less than three odorants with significant AUC (larger than 25% of the maximal AUC) were discarded. This exclusion criterion ruled out data from narrowly tuned recording sites, which provided only limited information on the relation between EOG and other measures. This exclusion criterion eliminated nine subjects, retaining 32 subjects for analysis. To calculate EOG distances, we represented each of the six EOGs as a vector in the time window of maximal activation within subject (see above). We then calculated the Euclidean distance between the EOG with maximal amplitude and the remaining five EOGs using the function 'pdist' (Matlab). Notably, the time window was subject specific. The average time window for this calculation was 700 ± 230 ms. EOG span was calculated as the maximal distance among all the pairwise EOG distances within subject.

Perceptual measures. Erratic perceptual measures were discarded (events in which the subject mistakenly did not use the scale bars or events in which the subject could not detect any odorant). This retained 927 out of 1,152 events in experiments 1 through 4 (experiment 5 was not used for correlational analyses, as it used only two odorants). We then calculated the subject mean pleasantness and intensity ratings. For each subject, we calculated the pleasantness distance between the odorant that elicited maximal EOG amplitude and the remaining five odorants, similar to the EOG distance calculation. Pleasantness span was the maximal pleasantness distance within subject, or in other words, the maximal range on a visual-analog scale used by a subject.

Chemical distances. To calculated the chemical distance between the odorant molecules, we downloaded their three-dimensional structures from PubChem and obtained their 1,491 physicochemical descriptor identity using Dragon Talete (http://www.talete.mi.it/index.htm). The Euclidean distance was calculated between the chemical identity vectors of any two odorants using the Matlab function 'pdist'. To calculate the odorant's distance in the first principal physicochemical axis, we performed principal component analysis on a comprehensive database of 2,993 odorant molecules. We then calculated the pairwise distances between our tested odorants using their projections on the first principal axis. For the optimized chemical distance, we used only the chemical descriptors previously identified as an optimized set[38] (**Supplementary Table 1**). For the individual chemical descriptors, we calculated the correlation between the chemical distances in each of the Dragon descriptors and the EOG distances, conditioned on that the descriptor distance distribution was normal (most were not).

Statistical analysis. To test for differences in the distribution of the above measures, we used two-way ANOVA interaction models. Moreover, to compare rank-ordering of responses across subjects we used Kruskal-Wallis tests. To test for differences across measures within subjects, we used paired student t-tests. Finally, correlations between measures (for example, **Figs. 5** and **6**) were computed using the Pearson correlation unless noted otherwise.

Optimizing a physicochemical metric for epithelial sorption. To test whether the EOG was tuned to mucosal sorption properties, we created an optimized descriptor metric based on bullfrog retention time (RT) values detailed in **Supplementary Table 2**. We downloaded from PubChem the three-dimensional structure of the molecules specified in **Supplementary Table 2** and obtained their chemical profile using Dragon Talete. We then applied a simple greedy algorithm that selected the chemical descriptors whose Euclidean distances correlated best with the pairwise log(RT) distances. The algorithm initiates by creating a null vector that represents the optimized weights of the chemical features that best describe the correlation between the chemical Euclidean distances and the log(RT) distances. At each iteration, each of the 1,491 chemical descriptors was added to the optimized chemical representation in turn. The Euclidean pairwise distances were calculated for each of these descriptors and the correlation between the chemical Euclidean distances and the log(RT) distances was derived. At the end of such a cycle, we have 1,491 correlation coefficients that represent

doi:10.1038/nn.2926

the contribution of each of the 1,491 descriptors to the chemical distance metric. The chemical descriptor with maximal correlation coefficient is added to the optimized weights vector. The cutoff criterion for stopping this optimization process is when the improvement in the correlation coefficient is smaller than 0.0001. Eventually, we ended with two chemical descriptors that best described the log(RT) distances: HATS2m (leverage-weighted autocorrelation of lag 2/ weighted by atomic masses) and RDF105m (radial distribution function – 10.5 / weighted by atomic masses) (for more information regarding these chemical descriptors see the Dragon user manual: http://www.talete.mi.it/help/dragon_help/index.html). This optimized metric was then used for calculation of the correlation between the retention-optimized chemical distance and the EOG distances.

Estimating odorant trigeminality. To test the trigeminality of the odorants, we asked ten subjects to localize the side of stimulation using a separated bi-nostril jar device[50]. The odorants were tested ten times each, five repetitions in each nostril. Maximum of five odorants were tested in each experiment. Each odorant was assigned a trigeminality score based on the localization accuracy (**Supplementary Table 3**). Ideally, this test would have been conducted under the same conditions as the EOG recordings, but the EOG olfactometer has only one line out, preventing localization studies. To address the possibility that judgment of non-trigeminality was biased by lower concentrations using the bi-nostril jar device, we used a photoionization detector (ppbRAE 3000) to measure concentration at the output points of the jars and the olfactometer (we tested set 3, which was least diluted). The jars always had a higher concentration (minimal increase 127%, maximal increase 35,714%), thus alleviating the concern of such bias. We stress, however, that many of these odors likely are trigeminal at higher concentrations than those used here.

Comparing perception following passive stimulation and active sniffing. To test whether the pleasantness estimates obtained during breath-holding in the EOG experiments were meaningful, we obtained repeated measures of pleasantness ratings under two conditions. conditions identical to the EOG experiment and conditions after sniffing the stimulus. The six odorants used for this experiment were from odorant set 2 (**Table 1**). Each odorant was presented three times with active sniffing and three times with breath-holding, summing to 36 fully randomized stimulus events (inter-stimulus interval = 45 s, stimulus duration = 500 ms, $n = 10$). No significant differences in perception were observed between the two conditions ($t_9 = 1.27$, $P = 0.20$), and the correlation in pleasantness perception across conditions was $r = 0.65$, $P < 10^{-7}$ (**Supplementary Fig. 2**).

50. Hummel, T., Futschik, T., Frasnelli, J. & Huttenbrink, K.B. Effects of olfactory function, age, and gender on trigeminally mediated sensations: a study based on the lateralization of chemosensory stimuli. *Toxicol. Lett.* **140–141**, 273–280 (2003).